Protein Engineering

DOI: 10.1002/anie.201204668

Unnatural Amino Acid Mutagenesis of Fluorescent Proteins**

Feng Wang, Wei Niu, Jiantao Guo, and Peter G. Schultz**

Fluorescent proteins are useful probes of protein localization and function both in vitro and in vivo.[1–3] As a result, considerable effort has focused on engineering new properties into fluorescent proteins.[1,4,5] Both directed evolution and rational design have resulted in mutant proteins with altered photophysical properties, stabilities, and sensitivity to pH value, exogenous ligands, phosphorylation and the like. To further explore the effects of steric/electronic perturbations to the fluorophore of a fluorescent protein, we previously substituted tyrosine 66 of the fluorophore in green fluorescent protein (GFP) with a series of unnatural amino acids.[6–8] Furthermore, others have reported the use of unnatural amino acid mutagenesis to study the spectral properties and folding behavior of GFP,[9] and to generate biosensors.[10,11] Herein we report the properties of four GFP (GFP_{UV}, a GFP variant optimized for maximal fluorescence when excited by standard UV light; Clontech) mutants in which the hydroxy substituent of Tyr66 is replaced with boronate, azido, keto, and nitro substituents (Scheme 1).

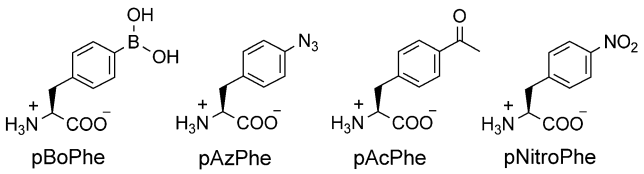

Scheme 1. The structures of the unnatural amino acids used herein.

The fluorophore of GFP is derived from cyclization of the Ser65-Tyr66-Gly67 tripeptide and, as a result, the phenolic side chain of Tyr66 forms part of the mature fluorophore. To replace Tyr66 with unnatural amino acids, orthogonal amber suppressor tRNA ($tRNA^{Tyr}_{CUA}$)/aminoacyl-tRNA synthetase (aaRS) pairs[6,12–14] with specificity for each of the unnatural amino acids (Scheme 1) were used to incorporate the unnatural amino acids in response to the amber nonsense codon. Mutant GFP_{UV} proteins (UFPs) containing different unnatural amino acids at position 66 were expressed in *E. coli* at 30 °C. The mutant proteins were purified by Ni^{2+} affinity chromatography with yields of isolated protein in the range of 4–107 $mg\,L^{-1}$ and characterized by mass spectrometry (Table SI1 and Figures SI1–SI5 in the Supporting Information). No fluorescence was observed for the Tyr66pBoPhe mutant (UFP-Tyr66pBoPhe). All other mutants displayed lowered relative fluorescence intensities and a shifted emission maximum (λ_{em}^{max}) compared to GFP_{UV} (Figure 1). UFP-Tyr66pNitroPhe (λ_{em}^{max} =510 nm) was the only protein with a red shift in λ_{em}^{max} relative to that of GFP_{UV} (λ_{em}^{max} =508 nm; Figure 1), and UFP-Tyr66pAcPhe (λ_{em}^{max} =442 nm) exhibited the most blue-shifted λ_{em}^{max} value among all four mutants. The quantum yields and extinction coefficients of these mutants are lower than those of GFP_{UV} (Table SI2 in the Supporting Information); this result may indicate that the packing of these mutant fluorophores inside GFP's β-barrel structure is less than optimal.

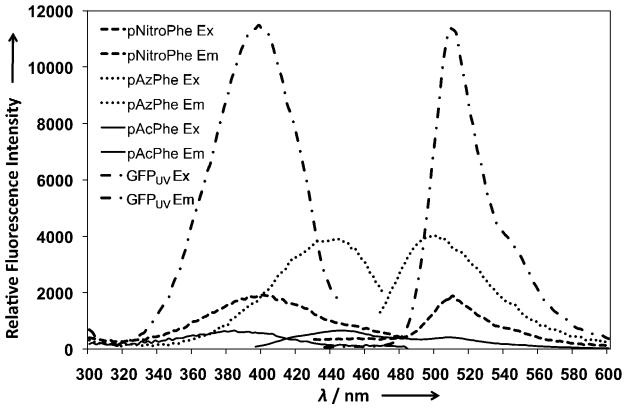

Figure 1. Fluorescence excitation (Ex) and emission (Em) spectra of GFP_{UV} and UFPs containing different unnatural amino acids at position 66. The λ_{em}^{max} values are 508, 498, 442, and 510 nm for GFP_{UV}, UFP-Tyr66pAzPhe, UFP-Tyr66pAcPhe, and UFP-Tyr66pNitroPhe, respectively. The λ_{ex}^{max} values are 395, 442, 384, and 400 nm for GFP_{UV}, UFP-Tyr66pAzPhe, UFP-Tyr66pAcPhe, and UFP-Tyr66pNitroPhe, respectively. Fluorescence spectra were measured in phosphate buffer (50 mM, pH 7.4), and emission spectra were recorded with excitation wavelengths of each fluorescence protein's λ_{ex}^{max}.

Previous studies have shown that arylboronate groups can be used to cage fluorescent molecules.[14] We expected a significantly lower fluorescence intensity of UFP-Tyr66pBoPhe, since the vacant 2p orbital of boron readily accepts electrons and makes the fluorophore more electron-deficient. Nevertheless, the complete loss of fluorescence of the protein is unexpected. Originally, we attributed this observation to

[*] Dr. F. Wang, Prof. P. G. Schultz
Department of Chemistry, The Skaggs Institute for Chemical Biology
10550 North Torrey Pines Road, La Jolla, CA 92037 (USA)
E-mail: schultz@scripps.edu
Dr. W. Niu, Prof. J. Guo
Department of Chemistry, University of Nebraska – Lincoln
Lincoln, NE 68588 (USA)
E-mail: jguo4@unl.edu

[**] This work is supported by grant DE-FG03-00ER46051 from The Division of Materials Sciences, DOE (P.G.S.), the Skaggs Institute for Chemical Biology (P.G.S.), and the New Faculty Startup Fund to J.G. from the Chemistry Department of University of Nebraska – Lincoln.

Supporting information (including materials and methods) for this article is available on the WWW under http://dx.doi.org/10.1002/anie.201204668.

the likelihood that the fluorophore of UFP-Tyr66pBoPhe is not fully matured. However, mass spectra analysis indicates that the fluorophore is formed (Figure SI1 in the Supporting Information). We next determined the X-ray crystal structure of UFP-Tyr66pBoPhe to 1.24 Å resolution (Figure 2A; data collection and refinement statistics are shown in Table SI3 in the Supporting Information). Consistent with the mass spectral results, the crystal structure shows that the fluorophore of UFP-Tyr66pBoPhe is completely formed (Figure 2A) and the overall structure of UFP-Tyr66pBoPhe is well aligned to that of a GFP variant (PDB: 1QYF; Figure SI6 in the Supporting Information). However, the *para*-boronate group is rotated by a small angle relative to the main plane of the fluorophore owing to the formation of hydrogen bonds to the backbone nitrogen of His148 and the hydroxy side chain of Ser205 (Figure 2A). Moreover, the bulky boronate side chain clearly pushes His148 away from the fluorophore (Figure 2A). This dislocation of His148, which has been shown to affect the conformational stability of the fluorophore,[15] could also attribute to the lack of any observed fluorescence.

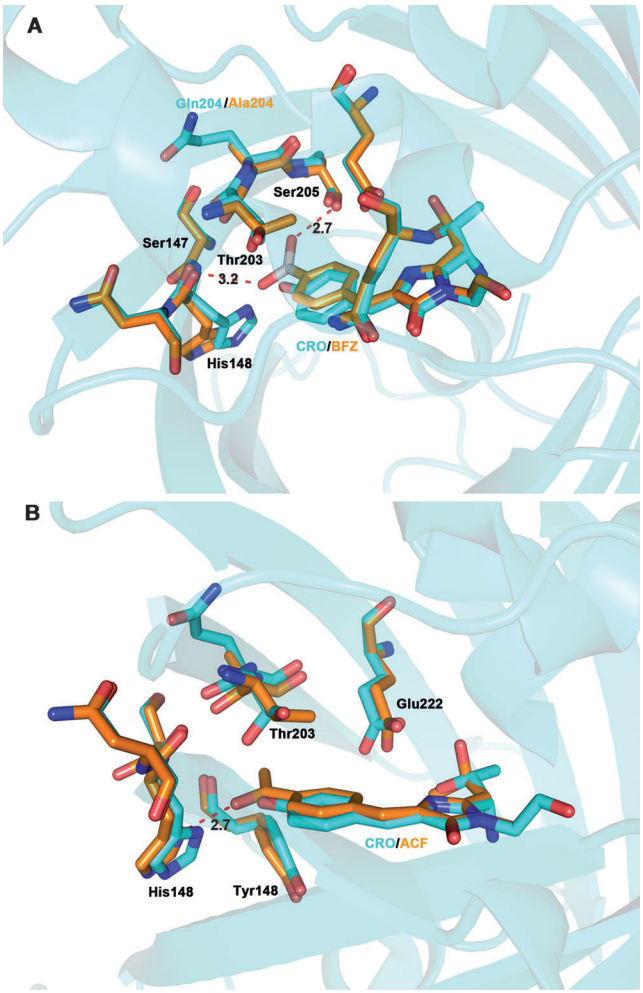

Figure 2. Crystal structures of UFP-Tyr66pBoPhe and UFP-Tyr66pAcPhe. A) Overlapped and expanded active-site structure of UFP-Tyr66pBoPhe (orange; fluorophore, BFZ) and a wt GFP variant (cyan; fluorophore, CRO; PBD: 1QYF). His-tagged UFP-Tyr66pBoPhe was crystallized to yield crystals that diffracted to 1.24 Å. The X-ray structure clearly shows the presence of the boronate group and cyclized fluorophore backbone; B) Overlapped and expanded active-site structure of UFP-Tyr66pAcPhe (orange; fluorophore, ACF) and a wt GFP variant (cyan; fluorophore, CRO; PBD: 1QYF). His-tagged UFP-Tyr66pAcPhe afforded crystals that diffracted to 2.0 Å. The X-ray structure clearly shows the presence of the acetyl group and cyclized fluorophore backbone.

Although the lack of fluorescence of UFP-Tyr66pBoPhe is unexpected, it provides us an interesting opportunity to engineer the fluorophore for biochemical applications. Arylboronate oxidation has been widely used as a reaction-based approach to H_2O_2 detection.[16] A few small-molecule fluorescent probes have been designed based on the chemoselective reaction of arylboronates with H_2O_2.[16] Inspired by this previous work, we hypothesized that the unique reactivity of pBoPhe towards oxidants might allow this mutant to be used as a chemical sensor, that is, pBoPhe can be converted to tyrosine upon oxidation[14] (Figure 3), which generates the fluorophore of GFP_{UV}. Indeed, after H_2O_2 treatment of UFP-Tyr66pBoPhe, strong fluorescence, which is identical to that of the GFP_{UV} (λ_{em}^{max} =508 nm), was observed (Figure 3A and Figure SI8 in the Supporting Information). Furthermore, the intensity of the fluorescence correlated well with the concentration of the oxidant (Figure 3B). The fluorescence was plotted versus the H_2O_2 concentration, and the obtained biphasic curve may result from the oxidation of GFP at higher concentrations of H_2O_2. Indeed, a decrease in fluorescence intensity was observed when GFP_{UV} was incubated with 100 mM H_2O_2 (Figure SI9 in the Supporting Information). In contrast, a nearly linear relationship was observed at lower concentrations of H_2O_2 (inset, Figure 3B). H_2O_2 detection in intact bacteria was also performed. An increase in fluorescence intensity was clearly observed when *E. coli* expressing UFP-Tyr66pBoPhe were incubated in phosphate buffer (50 mM) containing H_2O_2 (100 mM; Figure SI10 in the Supporting Information; because *E. coli* have significant catalase activity, a high concentration of H_2O_2 was required to attain a sufficient intracellular H_2O_2 concentration; *E. coli* are still viable after H_2O_2 treatment). As a control, no fluorescence intensity change was detected with native host *E. coli* in the presence of H_2O_2 (100 mM; Figure SI10 in the Supporting Information). Confocal fluorescence images also clearly showed that the oxidation of UFP-Tyr66pBoPhe by H_2O_2 can occur inside *E. coli* (Figure 3D). Because GFP can be genetically encoded, this approach may allow spatial resolution of redox chemistry when fused to a target protein of interest. In comparison to a reported genetically encoded H_2O_2 sensor, HyPer-2[17] (sixfold increase of the fluorescence intensity ratio F500/F420 in the presence of H_2O_2), the UFP-Tyr66pBoPhe displayed at least twentyfold improvement in dynamic range (Figure 3A). Finally, because the boronate group has a high affinity towards *cis*-diols, UFP-Tyr66pBoPhe may also be used as a carbohydrate sensor if a mutant of UFP-Tyr66pBoPhe can be generated such that the large carbohydrate molecule is accessible to the fluorophore.

The 66 nm shift in λ_{em}^{max} of UFP-Tyr66pAcPhe is the largest of the mutants. Previous studies on substituent effects of acetyl and hydroxy groups on small-molecule fluorophores show that the emission maximum of 1-acetylpyrene (406 nm)

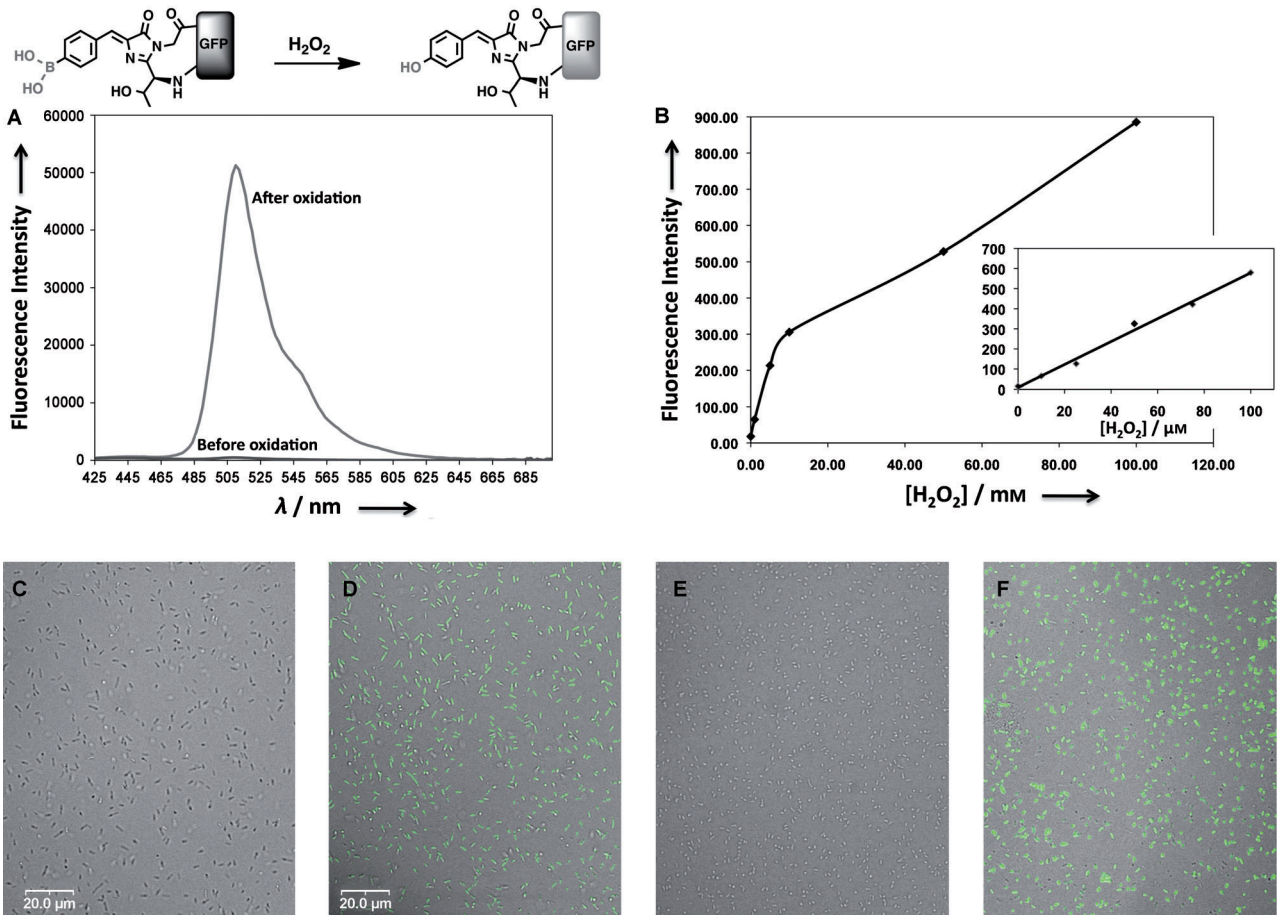

Figure 3. Oxidation of UFP-Tyr66pBoPhe. A) Fluorescence of UFP-Tyr66pBoPhe before (lower trace) and after (upper trace) H_2O_2 treatment; B) Changes in fluorescence of UFP-Tyr66pBoPhe after a incubation with different concentrations of H_2O_2 for 30 min; the inset shows the fluorescence changes of UFP-Tyr66pBoPhe after incubation with lower concentrations of H_2O_2 for six hours; C–F) Overlapped bright-field and fluorescence images of *E. coli*; C) *E. coli* expressing UFP-Tyr66pBoPhe before H_2O_2 (100 mM) treatment; D) *E. coli* expressing UFP-Tyr66pBoPhe after 15 min treatment with H_2O_2 (100 mM); E) *E. coli* only, after 15 min treatment with H_2O_2 (100 mM); F) *E. coli* expressing GFP_{UV}. The bright spots in (D) and (F) indicate the positions of GFP fluorescence.

is at a shorter wavelength than that of 1-pyrenolate (480 nm, in water) and at a longer wavelength than that of 1-hydroxypyrene (380 nm, neutral form in cyclohexane).[18,19] This finding is consistent with our observation that the anionic form of the GFP fluorophore emits at lower energy relative to that of the mutant fluorophore of UFP-Tyr66pAcPhe. In an attempt to further determine if other factors contribute to the significant blue shift in λ_{em}^{max} of UFP-Tyr66pAcPhe, we crystallized the protein and determined its X-ray crystal structure. The structure was solved at a resolution of 2.0 Å (Data collection and refinement statistics are shown in Table SI3 in the Supporting Information.). Based on the crystal structure, the fluorophore of UFP-Tyr66pAcPhe is completely formed (Figure 2B) and the overall structure of the protein remains the same as that of a wt GFP variant (Figure SI7 in the Supporting Information). However, the fluorophore of UFP-Tyr66pAcPhe does not overlap completely with that of the wt GFP variant (Figure 2B) as significant movements of surrounding amino acid side chains (His148, Tyr145, Thr203, and Glu222; Figure 2B) were clearly observed. This movement may arise from steric hindrance owing to a relative larger side chain of pAcPhe and the hydrogen-bonding interaction between the keto group of pAcPhe and His148 (Figure 2B). Moreover, this interaction locks the position of the ketone side chain of pAcPhe so that there is an angle of approximately 5° between the ketone group and the main plane of the fluorophore (Figure 2B). These interactions likely contribute to the large blue shift in λ_{em}^{max} and lower fluorescence quantum yield for this mutant.

In summary, we have site-specifically incorporated four unnatural amino acids into the fluorophore of GFP, and one of these mutants afforded a novel redox sensor. The fact that simple mutagenesis can be used to rapidly introduce unnatural fluorophores allows one to quickly generate fluorescent proteins with novel properties and functions.[7,8,10,11] Future efforts will focus on the design and synthesis of fluorescent proteins that can be used as other chemical sensors, for example, metal-ion sensors that can be derived from GFP mutants containing genetically-encoded metal-ion-chelating amino acids.

Received: June 14, 2012
Revised: August 9, 2012
Published online: September 5, 2012

Keywords: biosensors · fluorescence · fluorescent proteins · protein engineering · unnatural amino acids

[1] R. Y. Tsien, *Angew. Chem.* **2009**, *121*, 5721 – 5736; *Angew. Chem. Int. Ed.* **2009**, *48*, 5612 – 5626.
[2] C. D. Hu, T. K. Kerppola, *Nat. Biotechnol.* **2003**, *21*, 539 – 545.
[3] A. Miyawaki, *Annu. Rev. Biochem.* **2011**, *80*, 357 – 373.
[4] N. C. Shaner, P. A. Steinbach, R. Y. Tsien, *Nat. Methods* **2005**, *2*, 905 – 909.
[5] R. Heim, R. Y. Tsien, *Curr. Biol.* **1996**, *6*, 178 – 182.
[6] L. Wang, J. Xie, A. A. Deniz, P. G. Schultz, *J. Org. Chem.* **2003**, *68*, 174 – 176.
[7] D. Groff, F. Wang, S. Jockusch, N. J. Turro, P. G. Schultz, *Angew. Chem.* **2010**, *122*, 7843 – 7845; *Angew. Chem. Int. Ed.* **2010**, *49*, 7677 – 7679.
[8] D. D. Young, S. Jockush, N. J. Turro, P. G. Schultz, *Bioorg. Med. Chem. Lett.* **2011**, *21*, 7502 – 7504.
[9] N. Ayyadurai, N. S. Prabhu, K. Deepankumar, A. Kim, S. G. Lee, H. Yun, *Biotechnol. Lett.* **2011**, *33*, 2201 – 2207.
[10] N. Ayyadurai, P. N. Saravanan, K. Deepankumar, S. G. Lee, H. H. Jeong, C. S. Lee, H. Yun, *Angew. Chem.* **2011**, *123*, 6664 – 6667; *Angew. Chem. Int. Ed.* **2011**, *50*, 6534 – 6537.
[11] S. Chen, Z. J. Chen, W. Ren, H. Ai, *J. Am. Chem. Soc.* **2012**, *134*, 9589 – 9592.
[12] J. Chin, S. W. Santoro, A. B. Martin, D. S. King, L. Wang, P. G. Schultz, *J. Am. Chem. Soc.* **2002**, *124*, 9026 – 9027.
[13] L. Wang, Z. Zhang, A. Brock, P. G. Schultz, *Proc. Natl. Acad. Sci. USA* **2003**, *100*, 56 – 61.
[14] E. Brustad, M. L. Bushey, J. W. Lee, D. Groff, W. Liu, P. G. Schultz, *Angew. Chem.* **2008**, *120*, 8344 – 8347; *Angew. Chem. Int. Ed.* **2008**, *47*, 8220 – 8223.
[15] M. H. Seifert, J. Georgescu, D. Ksiazek, P. Smialowski, T. Rehm, B. Steipe, T. A. Holak, *Biochemistry* **2003**, *42*, 2500 – 2512.
[16] A. R. Lippert, G. C. Van de Bittner, C. J. Chang, *Acc. Chem. Res.* **2011**, *44*, 793 – 804.
[17] K. N. Markvicheva, D. S. Bilan, N. M. Mishina, A. Y. Gorokhovatsky, L. M. Vinokurov, S. Lukyanov, V. V. Belousov, *Bioorg. Med. Chem.* **2011**, *19*, 1079 – 1084.
[18] B. H. Milosavljevic, J. K. Thomas, *Photochem. Photobiol. Sci.* **2002**, *1*, 100 – 104.
[19] F. Hauke, A. Hirsch, S. Atalick, D. Guldi, *Eur. J. Org. Chem.* **2005**, *9*, 1741 – 1751.

